Analytical and Bioanalytical Chemistry
https://doi.org/10.1007/s00216-020-02723-4

RESEARCH PAPER

Probing high-affinity aptamer binding region and development of aptasensor platform for the detection of cylindrospermopsin

Raja Chinnappan[1] · Razan AlZabn[1] · Amjad K. Fataftah[1] · Ali Alhoshani[2] · Mohammed Zourob[1,3]

Received: 19 March 2020 / Revised: 7 May 2020 / Accepted: 18 May 2020

Abstract

Cylindrospermopsin (CYN) is one of the most concerning cyanotoxins due to its potential toxicity and spreading to various environments including drinking water. CYN has potential interferences with human and animal metabolic pathways, which influence the functions of organs including liver, kidneys, lungs, etc. CYN is involved in the inhibition of protein synthesis and detachment of ribosomes from the endoplasmic reticulum membrane. It also interacts with soluble proteins, which are associated with protein translations. It is believed that cytochrome 450 is responsible for the rapid toxicity of CYN. Researchers are urged to develop a high-throughput screening method for the detection of CYN in water. Construction of low cost, rapid, and sensitive analytical methods for the detection of CYN is challenging. Here, we used graphene oxide (GO) as the fluorescence sensing platform for probing the high affinity of the short aptamer derived from the wild-type long aptamer-CYN sensing. The biosensor construction involved two steps: first, quenching the fluorescence of fluorescent-labelled truncated aptamer using GO as a quencher and, second, fluorescence recovery in the presence of CYN by competitive binding between the target and GO. One of the truncate aptamers has a 12-fold higher affinity and enhances sensitivity compared to the long aptamer sequence. The limit of detection of the high affinity truncated aptamer is 17 pM which is 6-fold lower than the long aptamer (100 pM). The sensor specifically detects CYN in the presence of other potential interfering toxins. The performance of the sensor was validated using CYN spiked tap water with very good recovery percentage. A rapid and highly sensitive detection of CYN from water resources has been achieved using this method.

Keywords Bioanalytical method · Bioassays · Biosensors · Cylindrospermopsin

Introduction

Cyanobacteria are microorganisms that represent a threat to the biological community by the production of dense blooms, but most importantly by the production of cyanotoxins. One of these cyanotoxins is cylindrospermopsin (CYN). CYN is now considered the second most studied cyanotoxin worldwide as it is posing growing threats to human and environmental health [1, 2]. It has been reported previously that CYN is very stable with variable pH and temperature range and it is not decomposed when it is exposed to UV-visible light [3, 4]. The US Environmental Protection Agency has released the guideline value for CYN is 0.03 μg/kg/day [5]. Cylindrospermopsin is an alkaloid material made of a tricyclic guanidine coupled with hydroxymethyluracil. It is an ionic molecule with dipolar functional groups, which make it a highly water-soluble molecule [6]. Cylindrospermopsin and cyanobacteria capable of producing it are widespread throughout the world, making their detection of great importance. Many chromatographic techniques have been reported for the detection of CYN, including high-performance liquid chromatography coupled with different detecting systems like ultraviolet or mass spectrometry [1]. The use of high-performance liquid chromatography that has a photodiode array detector (HPLC-PDA) has been investigated as a detection method for the toxin [7]. Welker et al. (2002) evaluated the suitability of HPLC-PDA detection of CYN in environmental samples. They

Raja Chinnappan and Razan AlZabn contributed equally to this work.

✉ Mohammed Zourob
mzourob@alfaisal.edu

[1] Department of Chemistry, Alfaisal University, Al Zahrawi Street, Al Maather, Al Takhassusi Road, Riyadh 11533, Saudi Arabia

[2] Department of Pharmacology and Toxicology, College of Pharmacy, King Saud University, Riyadh 11451, Saudi Arabia

[3] King Faisal Specialist Hospital and Research Center, Al Zahrawi Street, Al Maather, Riyadh 12713, Saudi Arabia

Published online: 04 June 2020

tested several gradients and eluent pairs and found that the retention of CYN in C18 columns occurred only with gradients of acidified water and methanol [8].

Contamination of CYN in freshwater and fish muscle have been identified and quantitatively measured using liquid chromatography coupled to electrospray ion trap mass spectrometry (LC/ESI-MS/MS) [9]. The reported limit of detections (LOD) of CYN in the fresh water and the fish muscle were 0.10 ng/mL and 1.0 ng/g respectively. The low LOD values indicate the sensitivity method which could be applied for the monitoring the CYN contamination at early stages [9]. However, this method suffers from the low percentage recovery (63%) of the CYN. In another study, Blahova et al. have used immunochemical ELISA and liquid chromatography/mass spectrometry (LC/MS) method for the quantitative determination of CYN from various lake water samples [10]. The obtained results from the ELISA and LC/MS methods were comparable. However, the results confirmed that the LC/MS method is approximately 10-fold more sensitive (0.01–0.3 μg/L) than the ELISA method (0.4–4 μg/L). The matrix effect could be a possible reason for the differences in the sensitivity between the two methods [10].

Guzmán-Guillén et al. reported a novel method for the determination of cylindrospermopsin contamination in waters using solid-phase extraction (SPE), with graphitized carbon cartridges and quantified by liquid chromatography coupled with tandem mass spectrometry (MS). The limits of detection of this method was 0.5 μg/L, which is below the proposed guideline value of 1 μg CYN/L in natural waters [11]. Esterhuizen-Londt et al. reported a hydrophilic interaction liquid chromatographic-tandem mass spectrometric method, with a lower limit of detection of 200 fg on column (signal-to-noise ratio = 3, $n = 9$) and a lower limit of quantification of 1 pg on column (signal-to-noise ratio = 11, $n = 9$) [12]. Yen et al. (2011) reported the simultaneous determination of nine different cyanotoxins, including cylindrospermopsin, using a SPE-liquid chromatography (LC)-mass spectrometry (MS) in pure and natural waters. The authors reported detection limit between 2 to 100 ng/L by this method for total cyanotoxins in pure water. However, in the case of complexed water sample, the sensitivity of this system drop up to 10-fold [13].

Advances in nanotechnology led to the synthesis of a large number of nanomaterials with different structures and functions. These materials were applied in different areas such as energy [14, 15], electronics [16], environment, life sciences, and diagnostics [17–19]. Combined with the recognition ability of aptamer, these nanomaterials achieved high-performance biosensors based on optical detection or electrochemical measurements. Among them, graphene oxide (GO) attract tremendous attention because of its excellent fluorescence quenching properties, which make it a good material for the preparation of aptamer-based fluorescence quenching systems [20].

Single-stranded DNA, RNA aptamers specifically bind to the target molecules with high affinity (K_d in nanomolar to the picomolar range). Aptamers can bind to vide range of targets including metal ions [21], small organic molecules [22–24], proteins [25], bacteria [26], and viruses [27]. The systematic evolution of ligands by exponential enrichment (SELEX) method is applied to select the specific aptamer from the random sequence library containing 10^{15} oligonucleotides. In general, the aptamers contain 40–100 nucleotide bases. The ssDNA aptamer forms a unique complex secondary or tertiary structure to capture the target molecule to make a strong aptamer-target complex. The biosensors using aptamers as recognition receptor have many advantages over antibody-based sensors. Aptamers are more sensitive, thermally stable with a long life-time, small size, and of low production cost, as well as one can select the aptamer in vitro in the lab. Aptamer-based biosensors function from the change of aptamer conformation after the target recognitions, which then convert into the signal. Post SELEX modification of the long aptamer will enhance its performance significantly compared to an unmodified long aptamer [28–30]. The present study aims to develop a sensitive detection of CYN using high-affinity truncated aptamer associated with GO as a sensing platform.

This study aims to develop an aptamer-based biosensor for the sensitive detection of cylindrospermopsin, using high-affinity fluorescein truncated ssDNA aptamers and GO as a sensing platform. Recently, we have reported anti-CYN-aptamers having 60-nucleotide long with the affinity in the nanomolar range [31]. The high-affinity region of the long aptamer was screened by the systematic truncation method for the fabrication of robust biosensor to detect CYN. The specificity and the real sample validation have been tested.

Experimental

Materials and reagents

The cylindrospermopsin and other toxins, microcystin-LR (MC-LR), microcystin-YR (MC-YR), saxitoxin, anatoxin, and brevetoxins were purchased from NRC, National Research Council (Ottawa, Canada, www.nrc.canada.ca). Sodium chloride (NaCl), magnesium chloride ($MgCl_2$), *tris*(hydroxymethyl)aminomethane (Tris-base), boric acid, ethylenediaminetetraacetic acid (EDTA) disodium dehydrate, sodium azide, hydrochloric acid, and methanol were purchased from Sigma-Aldrich (St Louis, MO, USA). The mixture of 50 mM Tris (pH 7.4), 150 mM NaCl and 2 mM $MgCl_2$ is used as a binding buffer. The desalted unlabelled oligonucleotides and HPLC-purified labelled oligonucleotides (shown in Table 1) were purchased from metabion international (Planegg, Germany). All other chemicals were of analytical grade. The stock solution of cylindrospermopsin was

prepared in methanol and further dilutions were done in binding buffer. Milli-Q water with the resistivity of 18.2 MΩ cm at 25 °C was used to prepare DNA stock solutions and stored at − 20 °C until further use. The binding buffer was used for all the fluorescence and circular dichroism (CD) experiments. All the fluorescein-labelled probes were carefully protected from the light throughout the experimental procedures.

Instrumentation

NanoDrop 2000 (Thermo Scientific, Ottawa, Canada) UV-Vis spectrophotometer was used to determine the concentration of the DNA and protein. Fluorescence analysis for the fluorescein-labelled aptamers was achieved by using Nanodrop ND3300 fluorospectrometer (Thermo Scientific, Ottawa, Canada). The samples were excited in the light-emitting diodes (LEDs), $\lambda_{excitation} = 470 \pm 10$ nm, and the $\lambda_{emission}$ was monitored at 515 nm. Experiments were performed in triplicate unless otherwise mentioned. All the measurements were recorded in the binding buffer (pH, 7.4) at room temperature. The fluorescence spectra are the average of two measurements. Jasco J-815 CD Spectropolarimeter (Easton, MD, USA) was used for measuring the CD spectra over the wavelength range from 200 to 350 nm scanned at 2 nm min^{-1}. Two hundred microliters ultra-thin quartz cell was filled with the measuring solution. The concentration of aptamer and CYN in binding buffer was 2 μM and 5 μM respectively.

Screening aptamer binding region

The short binding region from the long parental aptamer of cylindrospermopsin has been screened in the present report. The 60-nucleotide anti-CYN-aptamer (Cy9) have been screened previously from our research group [20] with the dissociation constant of 89 nM for CYN. The affinity of the 60-nucleotide long aptamer towards the CYN is relatively good. However, only 20–40 nucleoids are directly associated with the binding of the target molecule. More number of random nucleotide sequences in the SELEX library favours the formation of more complexed secondary and/tertiary structure of the aptamer, which are believed to be the high-affinity binding regions and form strong complex with the target molecules [32, 33] On the other hand, the nucleotides which are not associated with the formation of complex structures (non-essential nucleotides) may not favour the aptamer-target binding [34, 35]. Therefore, removal of non-essential nucleotides in the long aptamer would facilitate its binding ability, sensitivity and sensing application. Fluorescence off/on was designed for probing the binding region having the essential nucleotides in the long aptamer. The approach employed here is based on the formation of strong aptamer-target complex in the presence of more folded form of aptamer. The FAM (6-carboxyfluorescein)-labelled truncated aptamers were used for probing the region. Graphene oxide was used as the quencher. The fluorescence of the truncated aptamer was quenched efficiently in the presence of GO. The sequences used in this study are tabulated in Table 1. The systematic slicing and labelling of the aptamer in different region and using GO as a sensing platform would lead to the finding of the binding region. Basing the secondary structure of the long aptamer in the physiological conditions from the mfold software leads to the successive truncation steps as shown in Fig. 1.

There are two major variants of the truncated aptamers that were designed and one of the high-affinity variants was further sliced into short sequences. The long aptamer has more complexed secondary structure as shown in Fig. 1, Cy9. The first truncated aptamer has 32 nucleotides with three stem-loop/bulges (Fig. 1(B) , Cy9T1) and 8 to 45 nucleotides from the 5′ end of the aptamer (the starting and ending red line in the Cy9, Fig. 1(A)). The second piece of short aptamer consists of 36 nucleotides, obtained by chopping the parental sequence at 16 and 49th positions from the 5′ end of the aptamer (Cy9T2, Fig. 1(C)). The resulting sequence has secondary structure with two stem/bulge and few unpaired nucleotides in bother ends as shown in Fig. 1. Cy9T2 was further reduced to 29 nucleotide sequences by removing the free unpaired nucleotides (Cy9T3, Fig. 1(D)). The Cy9T3 secondary structure (Fig. 1(D)) is similar to Cy9T2 except for the flanking nucleotide in both edges. The bulge between the stems in Cy9T3 was removed by eliminating 6 nucleotides which form the bottom stem, leading to single stem-loop structure (Cy9T4, Fig. 1(E)). All the short truncated aptamers were FAM labelled at 5′ end and used for the sensor application using GO as a sensing platform.

Table 1 Original and truncated aptamers sequences used in the work

Name	Sequence from 5′ to 3′
Cy9FAM	FAM-5′GGCATCAGGCAACAACCGATGGTCCGGCCACCCTAACAACCAGCCCACCCACCACCCCGCCG-3′
Cy9T1FAM	FAM-5′GGCAACAACCGATGGTCCGGCCACCCTAACAACCAGCCCACC-3′
Cy9T2FAM	FAM-5′CCGATGGTCCGGCCACCCTAACAACCAGCCCACCCA-3′
Cy9T3FAM	FAM-5′CCGATGGTCCGGCCACCCTAAC-3′
Cy9T4FAM	FAM-5′GGTCCGGCCACCCTAACAACCAGCCCACC3′

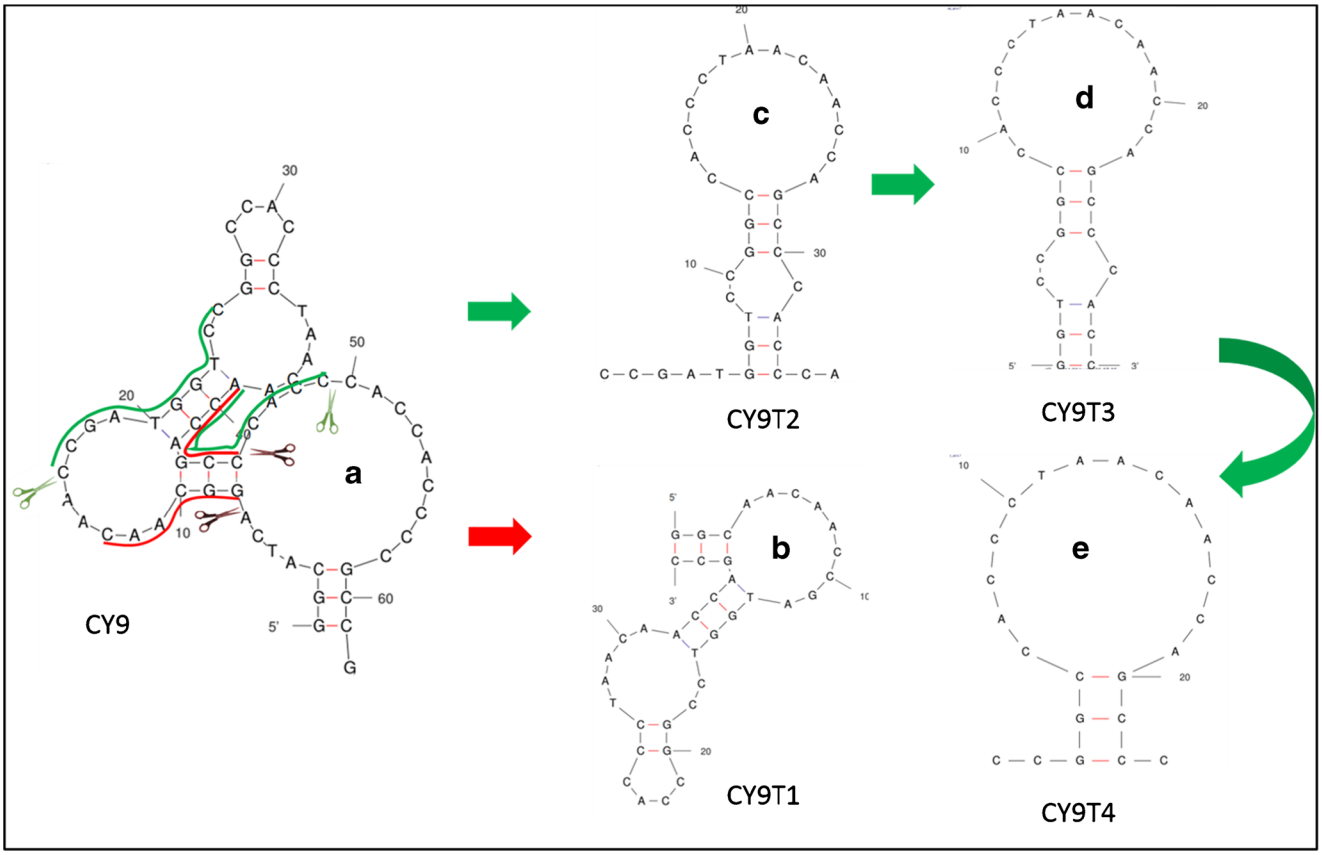

Fig. 1 (A) Secondary structure of full-length TM aptamer. (B) Secondary structure 38 nucleotide truncated aptamer (Cy9T1). (C) Secondary structure of 36 nucleotide truncated aptamer (Cy9T2). (D) Secondary structure of 29 nucleotide truncated aptamer (Cy9T4). (E) Secondary structure of 23 nucleotide truncated aptamer (Cy9T4)

Optimization of graphene oxide/aptamer ratio and detection

As graphene oxide (GO) an efficient fluorescence quencher, it is used as a sensing platform by switching the fluorescence signal from off to on state in the presence of CYN. The concentration of fluorescent aptamer was optimized from the detectable fluorescence signals with a decent signal to noise ratio in the presence of GO. The concentration ratio of GO to aptamer was optimized by titrating the fixed amount (25 nM) of fluorescently labelled aptamer with an increasing amount of GO in the dynamic range of 0–50 μg/mL in binding buffer at pH 7.4. The aptamer-GO samples were kept at room temperature for 30–35 min to facilitate the maximum number of aptamer adsorbed of the surface of the GO sheet. Variable concentrations of CYN in the range of 0.01 to 40 nM were added to the solution of optimized aptamer to GO ratio (25 nM aptamer for 15 μg/mL). The samples in binding buffer were incubated at room temperature for 30 min to form a stable aptamer-CYN complex. The fluorescence intensity of each sample was measured at 515 nm by exciting the samples in the wavelength of 470 ± 10 nm. The measured fluorescence values were plotted against the corresponding concentration of GO used (Fig. 2).

Specificity and validation of aptasensor

The selective binding of CYN by the truncated aptamer, Cy9T2, was tested using the GO-aptasensor. A number of marine toxins associated with CYN such as microcystin-LR, microcystin-YR, brevetoxin, anatoxin, and saxitoxin have been tested. The sensor was treated with 25 nM solution of each toxin individually and the corresponding fluorescence intensities were measured. The percentage change in the fluorescence signal of each sample was compared with CYN, which represents the extent of cross-reactivity with the truncated aptamer.

The aptasensor developed was validated by spiking CYN in tap water. Different concentrations of (0.5, 2, and 10 nM) of CYN were spiked and incubated with the sensor. The fluorescence intensities of each sample were compared with the standard calibration plot to calculate the percentage recovery (Table 2).

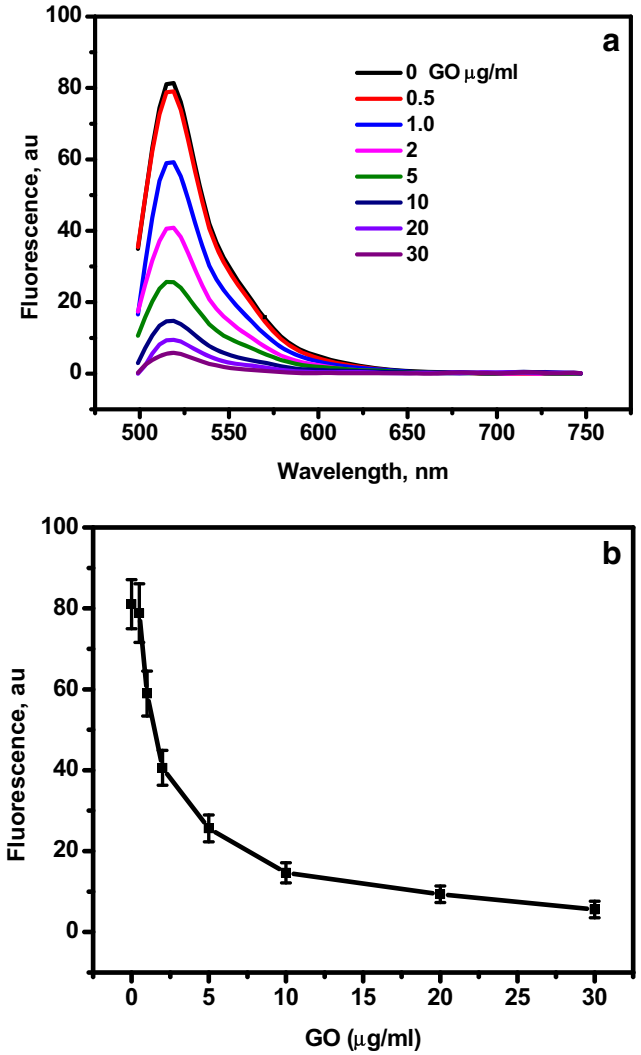

Fig. 2 **a** Fluorescence intensity of Cy9T2 (25 nM) with increasing concentration of graphene oxide (GO). **b** Plot of GO concentration vs fluorescence intensity of Cy9T2 at 515 nm (λ-max). The fluorescence spectra were recorded by exciting at 470 ± 10 nm and the emission intensity 515 nm was used for the plots. The error bars represent the standard deviation of three different measurements

Results and discussion

The process of SELEX uses diverse DNA library sequences for the in-vitro screening. The most common aptamer contains typically 40–100 nucleotides. The longer the oligonucleotide sequences, the more the diversity in the library sequences, which eventually enhances the probability of complex structure as the result selection of high affinity and selective/specific aptamer against the target molecule. Though the long aptamer has relatively high affinity and specificity, not all the sequences in the aptamers are playing a significant role in the target binding. Therefore, post SELEX modification of long aptamer is important to fabricate sensitive and specific biosensor platform. The long aptamers are divided into three different regions based on their functions, essential region, non-essential region, and supporting region. The essential region is in contact with the target molecule and any modification in this region leads to the loss of its binding ability. The supporting nucleotides are important for the formation of a secondary structure and help to keep the aptamer-analyte complex stable. The non-essential nucleotides inhibit the rest of the nucleotides to form aptamer-target complex. The conserved region of aptamers mainly have stem-loop, G-quadruplex, pseudoknot, budge in the stem, and more junction structures. The aptamer with a linear structure might favour the target binding. The non-essential region of the sequences may form a secondary structure with the essential nucleotides, inhibits the functions of the essential region, and averts the target binding.

In addition to the high affinity of short aptamer, the fabrication of biosensing platform with large-sized aptamer is not favourable. Moreover, in most of the biosensing approaches, the signal generation is mainly by short-sequence structure switching mechanisms and short sequences reduce the cost of production. Therefore, identification of the high-affinity region and fabrication of biosensor with the potential aptamer would facilitate the sensitive detection of target analytes.

Our research group has reported the selection of high-affinity aptamer against CYN with the length of 96-nucleotide from the 1.5×10^{15} diverted library single-stranded DNA sequences recently by in vitro selection method. Most of the selected aptamer have a good binding affinity for CYN in the range of nanomolar levels. One aptamer has the dissociation constant of 88 nM, and though it is decent, the length of the aptamer would obstruct its functions. Slicing out the obstructing region by truncation would improve the binding ability and specificity as well as designing the biosensor in multivalent function for the robust detection of the target analytes.

Table 2 Application of Cy9T2 sensor duplex for the detection of CYN in water sample

Spiked Conc (nM)	Calculated Conc (nM)	Recovery (%)	STD
0.5	0.46	92	± 4.7
2	2.46	123	± 10.4
10	9.6	96	± 5.3
30	29.49	98.3	± 3.5

High-affinity aptamer truncation design

The full-length Cy9 aptamer selected was used for the truncation study. The secondary structure of the aptamer in the physiological conditions (50 mM Tris + 150 mM NaCl + 2 mM MgCl2, pH 7.4) was obtained from the mfold software as shown in the Fig. 1(A), Cy9. The systematic truncation of the aptamer was made based on the secondary structure of

the long original aptamer. The long aptamer was truncated into two major parts, the first one is obtained by trimming 8 nucleotide from 5′ end and 17 nucleotides from 3′ end (Cy9T1, Fig. 1(B)). The nucleotide bases in the resulting aptamer forms complex secondary structure. The eliminated nucleotides were swinging on both sides, not forming much complex structure, and were assumed that these are probable loss for the associated target binding. Cy9T1 was labelled with FAM at the 5′ ends and also the GO-based fluorescence assay as described in the "Optimization of graphene oxide/aptamer ratio and detection" and "Specificity and validation of aptasensor" sections. No significant increase in the fluorescence intensity by the addition of a large amount of CYN was observed. The results show that Cy9T1 aptamer did not disturb the π-π stacking interaction between the GO sheet and Cy9T1 and detach from the GO surface in the presence of CYN. It indicates that Cy9T1 aptamer is missing some essential nucleotides, which are removed either from 5′ or 3′ end. As there are only a few nucleotides that have been omitted from 5′ end, we assume that the nucleotides from 3′ would be important for binding. Therefore, we used another strategy for the second truncation by adding more nucleotides in the 3′ end and removing 8 nucleotides from the 5′ end of Cy9T1, resulting to 33 nucleotide short aptamers with the structure (Cy9T2) as shown in Fig. 1(C). Cy9T2 was FAM labelled and tested with GO-based fluorescence assay. In the presence of the target molecule, the fluorescent aptamer detached from the surface of the graphene oxide sheet and bind to the target molecule by switching its conformation. The surface detachment and conformation switching were monitored by a significant increase in the fluorescence signal. The results indicate that this part of the aptamer region with the given conformation is a more favourable form for target binding. In order test the binding ability of the short aptamer from Cy9T2, we cut off the five and two hanging nucleotides in 5′ and 3′ ends respectively; the resulting structure is similar to Cy9T2 without the hanging part (Cy9T3, Fig. 1(D)). FAM-labelled Cy9T3 was tested with GO-based fluorescence sensor in the presence of CYN, resulting in only background signal. No fluorescence signal indicates that the flanking nucleotides in both ends are supporting nucleotides, which are crucial for the aptamer-target complex formation. Though they are not involved in the secondary structure formation, presumably, they assist the target to bringing closer to the essential nucleotides and form a unique binding pocket for CYN, thereby facilitating and stabilizing the complex. Just for curiosity, we remove the bulge from Cy9T3 by removing the three nucleotides from both sides leading to stem-loop structure (Cy9T4, Fig. 1(E)) and conducted a test. There is no change in the fluorescence in the presence of CYN, indicating that short aptamer lost its binding ability. The nucleotides swinging on both sides of the target have been tested against the target molecule; however, there is no change in the fluorescence signal in the presence of the target, indicating that there is no binding between the aptamer and the target. Results were not included since the signals are unchanged by the addition of target molecules. Finally, the binding region of the long aptamer for CYN is found to be Cy9T2 with stem-loop and a binge in the stem with hanging unpaired nucleotides and is used for further studies.

Graphene oxide as a biosensor platform

Graphene oxide is a multiple layer of a two-dimensional aromatic structure with honeycomb sheet structure with unique electronic, thermal, and optical properties. Due to its unique nature, it acts as an efficient quencher up to the distance of 300 A° and also a strong acceptor for the fluorescence resonance energy transfer (FRET) in the whole spectrum of the visible region. GO is known to have surface adsorption nature of biomolecules such as DNA, RNA, bacteria, and small organic molecules. GO is a strong fluorescence quencher than the common organic quencher molecules and it absorbs the fluorescent photons by FRET mechanism. It is known that GO interacts with ssDNA by non-covalent π-π stacking and hydrophobic interactions, therefore the fluorescence of the fluorescent-labelled ssDNA was used to make off state. The Cy9T2 has high fluorescence change in the presence of target; we selected this aptamer for GO-based fluorescence stature switching assay. This assay is associated with two major parts. The first part is to create the fluorescence off state by quenching the fluorescence of labelled Cy9T2 aptamer. The second part is to recover the quenched fluorescence (on stare) of labelled aptamer by introducing the target, CYN. As shown in Scheme 1, the amount of aptamer-CYN complex is related to change in the fluorescence intensity, which is directly proportional to the amount of CYN present in the solution.

Optimization of GO-aptamer ratio by fluorescence quenching

The optimization of the assay was done by finding the maximum fluorescence quenching of FAM-Cy9T2 in the presence of minimum amount of GO and the fluorescence intensity has a significant signal to noise ratio (s/n). The optimized amount of (25 nM) FAM-Cy9T2 is used for further experiments. A constant amount of Cy9T2 was titrated against variable concentrations of GO (0 to 30 μg/mL). Cy9T2 has strong fluorescence in the absence of GO; however, by adding GO, the fluorescence signal starts to reduce gradually with increasing concentration as shown in Fig. 2a. More than 95% of the fluorescence was quenched in the presence of 30 μg/mL of GO, indicating that most of the fluorescent aptamers are adsorbed on the GO surface. While exciting the fluorescent aptamer, the energy of the fluorescence is transferred to GO by FRET. As depicted in Fig. 2b, the fluorescence intensity

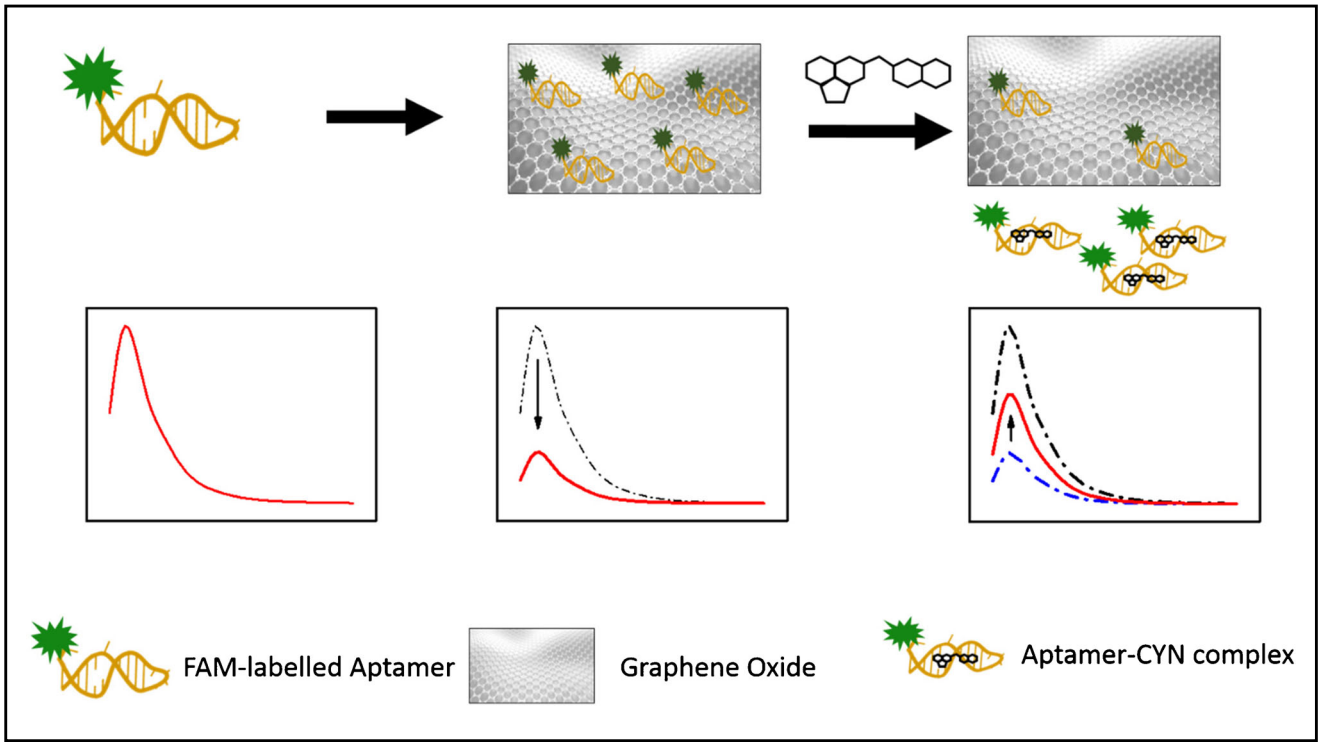

Scheme 1 The fluorescence switching in graphene oxide-based fluorescence assay for cylindrospermopsin. Stage 1: The free aptamer has a high fluorescence signal. Stage 2: The fluorescence was quenched by the presence of graphene oxide. Stage 3: introduction of target sample and the aptamer detached from the GO surface and complexed with the target with high affinity, resulting to the increase of the fluorescence signal

against GO concentration plot shows that more than 80% of the fluorescence was lost in the presence of 15 μg/mL of GO. We selected the optimal amount of GO at which ~ 80–85% quenching occurs, and to avoid any false results we made sure all the aptamers are adsorbed on the GO surface. The concentration ratio of 25 nM of Cy9T2 for 15 μg/mL is considered as fluorescence off state and the rest of the experiments have been done at this condition.

Determination of dissociation constant of Cy9T2

As Cy9T2 undergoes conformation change in the presence of the target, the dissociation constant of Cy9T2 aptamer for CYN was determined by the GO-based fluorescence method. The off state of the sensor platform was prepared as described above (25 nM of Cy9T2 for 15 μg/mL) and was used for the K_d measurements. Different concentrations of CYN were incubated in the dynamic range of 0–50 nM with a constant amount of aptamer-GO mixture. After 30 min, the fluorescence was recorded and plotted against the corresponding CYN concentrations. The dissociation constant of the aptamer was obtained by fitting the plot using nonlinear regression analysis (Fig. 3). The dissociation constant of Cy9T2 was found to be 7.4 nM, which is 12-fold higher than the long parental aptamer (89 nM). The results indicate that the truncated short aptamer obtained by the removal of non-essential nucleotides forms a more stable complex with CYN with high affinity. Our previous truncation studies showed that the short aptamers have significant improvements in their affinity in comparison with the respective long sequences [25, 28–30, 36].

Aptamer-based fluorescence assay for CYN detection

The aptasensor developed for the detection of CYN using short truncated aptamer was established using GO as a sensing platform. Initially, the fluorescence off state was optimized as described in the "Optimization of GO-aptamer ratio by fluorescence quenching" section. The fluorescence of the FAM-labelled aptamer is used as a probe for the detection of CYN. To determine the limit of detection, different concentrations of CYN were added to the GO-aptamer mixture. As shown in Fig. 4, the fluorescence intensity increases linearly with increasing the concentrations of CYN and more than 45% of the FAM fluorescence was recovered in the presence of 50 nM concentration of CYN. The CYN molecule triggers the aptamer detachment from the GO surface. Due to the high affinity of CYN with the aptamer, it could destabilize the GO-aptamer π-π stacking interaction and form strong complex. Once the CYN-aptamer complex is formed, it is released to the solution and there is no close interaction with the GO, and as a result, the fluorescence intensity recovered from the GO quenching. The recovered fluorescence signals were plotted

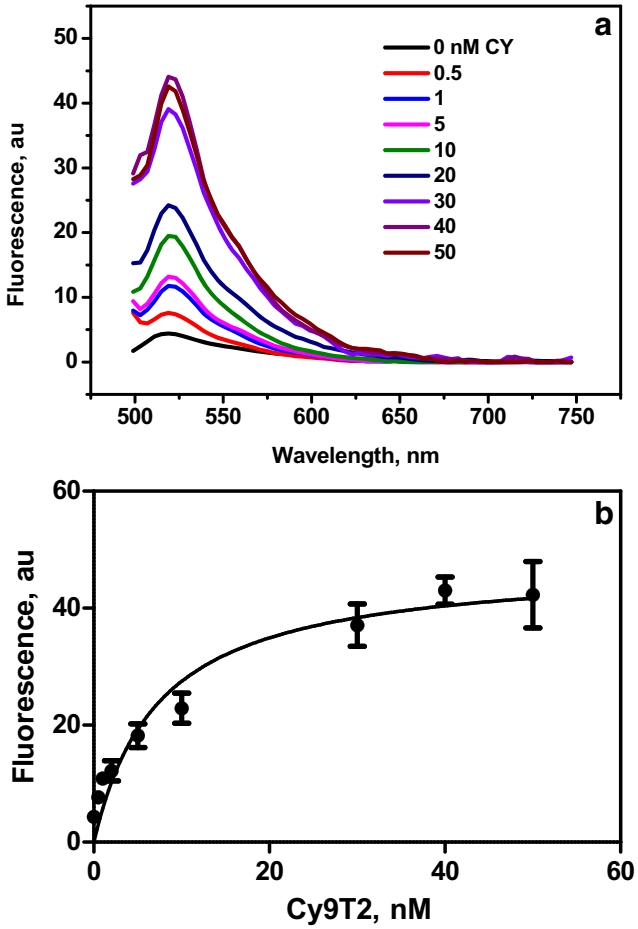

Fig. 3 **a** Aptamer release from the GO surface by the addition of cylindrospermopsin. Increase in the fluorescence intensity with increase in the concentration of CYN. **b** Saturation binding affinity curve obtained from the titration of CYN with GO-Cy9T2 aptamer. The error bars represent the standard deviation obtained from three different measurements. The fluorescence spectra were recorded by exciting at 470 ± 10 nm and the emission intensity 515 nm was used in the graph. The error bars represent the standard deviation of three different measurements

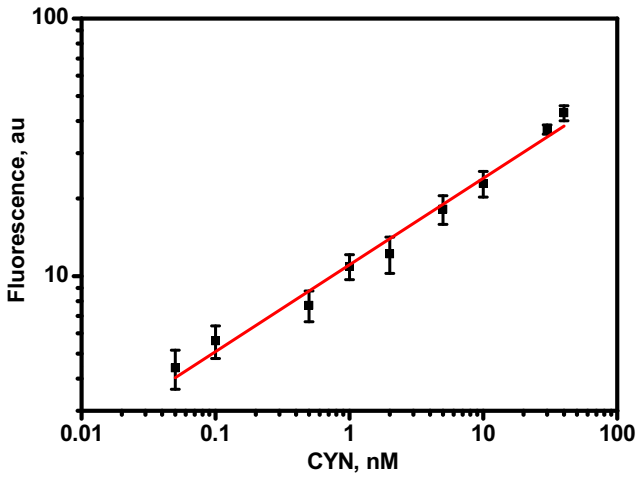

Fig. 4 The calibration plot fluorescence intensity of Cy9T2 against the concentration of CYN at 515 nm. The fluorescence spectra were recorded by exciting at 470 ± 10 nm and the emission intensity 515 nm was used for the plots. The error bars represent the standard deviation of three different measurements

against the corresponding concentrations to generate a calibration curve to calculate the limit of detection. As shown in Fig. 4, the linear relationship between the fluorescence intensity and the respective concentrations were observed. The LOD was calculated from the following equation LOD = 3.3 SD/*s*, where SD is the standard deviation of the signal in the absence of cylindrospermopsin and *s* is the slope obtained from the linear calibration curve. The Cy9T2 has the LOD of 17 pM, which is 6-fold lower than the LOD of long aptamer reported before [20]. The improvement of the sensitivity of the short aptamer is possibly due to the elimination of non-essential region of the aptamer, which might prevent the formation of the secondary and tertiary structure of the aptamer to have a unique binding pocket for the CYN binding. Unlike small molecules, designing the GO-based aptasensor is quite possible for the large molecules and proteins [25, 36]. It is a challenging task to find the binding region of the small molecule by GO-based method. In the case of large molecules, the aptamer binding pocket might be buried in the molecule and can easily interrupt the physical adsorption of the aptamer on the GO surface. However, in the case of small molecule, unless the labelled nucleotide is directly associated with the target binding, it may not detach from the GO surface. We could see the significant signal enhancement by small CYN molecule, indicating that the FAM-labelled nucleotide is strongly associated with aptamer-CYN complex formation. The aptamer response as the measure of fluorescence intensity in the presence of a fixed amount of CYN is shown in Fig. 5. Electrochemical impedimetric aptasensor for the detection of trace amount of CYN has been fabricated using amine aptamer grafted on thionine-graphene surface. The change in the conformation upon CYN binding is monitored. This method could detect as slow as 0.117 ng/mL of CYN [37], which is comparable to our method. Recently, a novel N8 anti-CYN monoclonal antibody was produced which has high affinity compared to other antibodies. Direct competitive time-resolved fluorescence immunoassay (TRFIA) was used for the detection of CYN. This technique could detect as low as 0.02 ng/mL of CYN [38]. Díez-Quijada el al. have reported the detection of CYN in the lettuce matrixes. In this method, a solid-phase extraction (SPE) system was used for the extraction of toxin and ultra-performance liquid chromatography-tandem mass spectrometry (UPLC-MS/MS) was used for the quantification and analysis. The lowest detection limit for this method is 0.07 ng/mL [38]. TRFIA and UPLC-MS/MS detection methods have high sensitivity compared to our method; however, TRFIA is an antibody-based method which has certain limitations such as production of an antibody by sacrificing animals, thermal unstability, and high cost. The UPLC-MS/MS method is associated with highly expensive

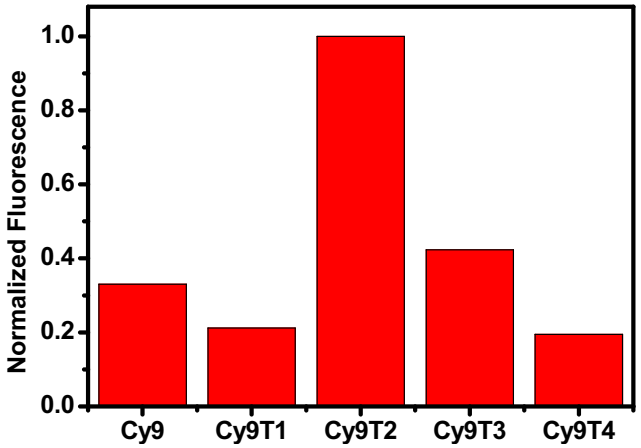

Fig. 5 The fluorescence measurement results of the different truncated aptamers used in the GO-based aptasensor at fixed concentration of CYN. The fluorescence spectra were recorded by exciting at 470 ± 10 nm and the emission intensity 515 nm was used for the plots

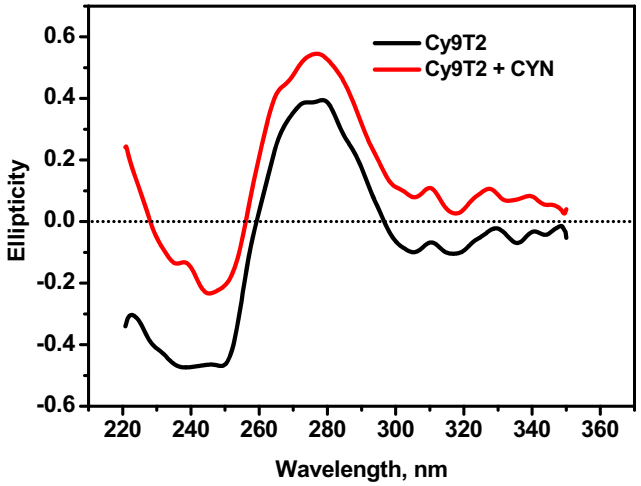

Fig. 6 CD spectroscopy analysis of 2 μM concentration the Cy9T2 aptamer before and after incubation with 5 μM concentration of the CYN target molecule

sophisticated instruments such as solid-phase extraction, UPLC, and mass spectrometry. According to the WHO, the guideline value of CYN in human drinking water is 1 μg/L. The LOD of our method is much lower than the guideline value, and therefore, we are confident that our method will be used for the real sample analysis. From the results, the truncated aptamer is much more sensitive for the detection of CYN. The optimization of GO-aptasensor would be an ideal robust sensor platform for the sensitive detection of CYN from various matrixes.

Circular dichroism studies

Circular dichroism studies provide the structure switching conformation change upon the target interaction with the aptamer. The involvement of nucleotides in the short aptamer for the target binding was tested by the change in the pattern of the CD spectrum. As shown in Fig. 6, there is a significant change in the CD spectrum in the presence of CYN. In the absence of the target, Cy9T2 has a single peak at 270 nm; however, the shape of the aptamer-CYN complex spectrum has changed to S-shaped with two peaks at 270 and 240 nm respectively. The magnitude of change in ellipticity is the measure of conformation change in the aptamer and the stability of the aptamer-target complex. The results indicate that the 33mer short aptamer has better binding ability compared to the parent aptamer.

Cross-reactivity and specificity

The selective binding of the Cy9T2 aptamer with CYN is tested by the aptasensor from the fluorescence response using different molecules that are closely associated with CYN. Brevetoxin, microcystin-LR, YR, saxitoxin, and anatoxin-A and CYN were incubated individually with the aptasensor. The change in the fluorescence of 25 nM solution from each analyte is monitored and represented as a bar graph as shown in Fig. 7. The significant increase in the fluorescence intensity induced by CYN is normalized to 100% and other fluorescence values were compared with this. Microcystin-LR and saxitoxin have cross-reactivity of about 25 and 20% respectively. The rest of the biotoxins showed no significant increase in the fluorescence signals indicating that the aptamer is selectively bound to CYN and not to the other biotoxins. The newly designed sensor would be applied for the detection of CYN selectively from the mixture of other associated biotoxins.

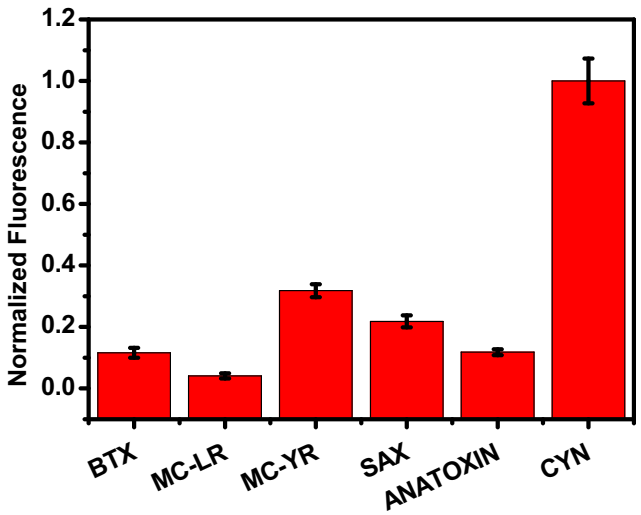

Fig. 7 The cross-reactivity response of GO-Cy9T2 aptamer (15 μg/mL–25 nM) fluorescence assay for different toxin samples concentrations of 25 nM, cylindrospermopsin (CYN), brevetoxin (BTX), microcystin-LR (MC-LR), microcystin-YR(MC-YR), saxitoxin (SOX), and anatoxin-A (AXA). The fluorescence intensity of each sample obtained by exciting at 470 ± 10 nm and the emission intensity 515 nm was used in the graph. The error bars represent the standard deviation of three different measurements

Real sample analysis

At the end, the performance of the proposed sensor with the short aptamer was tested with the water samples. Three different concentrations of CYN were spiked with the tap water and incubated with the sensor. The change in the fluorescence was measured and compared with the calibration curve. The percentage recovery of CYN from the samples are tabulated in Table 2. The spiked and the recovered values are close to each other, indicating that the sensor is functioning well without any interference from the other molecules/ions in the tap water. The results are supportive of the use of the sensor to test CYN in the contaminated water sources.

Conclusions

This is a simple aptamer truncation to identify the short binding region of the long aptamer selected from the SELEX process. The parent aptamer is divided into various segments and each one was labelled with FAM at the 5′ end, and GO-based aptasenors were developed and tested against CYN. One of the 33mer aptamer showed 12-fold high affinity and 6-fold lower detection limit in comparison with the wild-type original aptamer. The CD spectrum also supports the conformation change upon the target binding. The detection limit of the aptamer has been enhanced by 6 folds. The aptamer has high selectivity against the other interfering biotoxins and robust function in real samples. This mapping method would be applied for the other long aptamer to identify the core binding region for efficient signal enhancement. The CYN recovery from the water reveals the potential application of the sensor for the food and environmental sample analysis.

Acknowledgements The authors would like to acknowledge the funding from the research office at Alfaisal University.

Compliance with ethical standards

Conflict of interest The authors declare that they have no conflict of interest.

Research involving humans and animal rights This research did not involve human participants and/or animals.

References

1. Moreira C, Azevedo J, Antunes A, Vasconcelos V. Cylindrospermopsin: occurrence, methods of detection and toxicology. J Appl Microbiol. 2013;114:605–20.
2. Armah A, Hiskia A, Kaloudis T, Chernoff N, Hill D, Antoniou MG, et al. A review on cylindrospermopsin: the global occurrence, detection, toxicity and degradation of a potent cyanotoxin. Environ Sci Process Impacts. 2013;15:1979–2003.
3. Chiswell RK, Shaw GR, Eaglesham G, Smith MJ, Norris RL, Seawright AA, et al. Stability of cylindrospermopsin, the toxin from the cyanobacterium, cylindrospermopsis raciborskii: effect of pH, temperature, and sunlight on decomposition. Environ Toxicol. 1999;14:155–61.
4. Wörmer L, Huerta-Fontela M, Cirés S, Carrasco D, Quesada A. Natural photodegradation of the cyanobacterial toxins microcystin and cylindrospermopsin. Environ Sci Technol. 2010;44:3002–7.
5. Farrer D, Counter M, Hillwig R, Cude C. Health-based cyanotoxin guideline values allow for cyanotoxin-based monitoring and efficient public health response to cyanobacterial blooms. Toxins. 2015;7:457–77.
6. Ohtani I, Moore RE, Runnegar MTC. Cylindrospermopsin: a potent hepatotoxin from the blue-green alga Cylindrospermopsis raciborskii. J Am ChemSoc. 1992;114:7941–2.
7. Hiskia A, Spoof L, Kaloudis T, Meriluoto J. Determination of cyanotoxins by high-performance liquid chromatography with photodiode array. Handbook of cyanobacterial monitoring and cyanotoxin analysis, 2017, 205.
8. Welker M, Bickel H, Fastner J. HPLC-PDA detection of cylindrospermopsin—opportunities and limits. Water Res. 2002;36:4659–63.
9. Gallo P, Fabbrocino S, Cerulo MG, Ferranti P, Bruno M, Serpe L. Determination of cylindrospermopsin in freshwaters and fish tissue by liquid chromatography coupled to electrospray ion trap mass spectrometry. Rapid Commun Mass Sp. 2009;23:3279–84.
10. Blahova L, Oravec M, Maršálek B, Šejnohová L, Šimek Z, Bláha L. The first occurrence of the cyanobacterial alkaloid toxin cylindrospermopsin in the Czech Republic as determined by immunochemical and LC/MS methods. Toxicon. 2009;53:519–24.
11. Guzmán-Guillén R, Prieto AI, Gonzalez AG, Soria-Díaz ME, Cameán AM. Cylindrospermopsin determination in water by LC-MS/MS: optimization and validation of the method and application to real samples. Environ Toxicol Chem. 2012;31:2233–8.
12. Esterhuizen-Londt M, Kühn S, Pflugmacher S. Development and validation of an in-house quantitative analysis method for cylindrospermopsin using hydrophilic interaction liquid chromatography–tandem mass spectrometry: quantification demonstrated in 4 aquatic organisms. Environ Toxicol Chem. 2015;34:2878–83.
13. Yen H-K, Lin T-F, Liao P-C. Simultaneous detection of nine cyanotoxins in drinking water using dual solid-phase extraction and liquid chromatography–mass spectrometry. Toxicon. 2011;58:209–18.
14. Wei D. Writable electrochemical energy source based on graphene oxide. Sci Rep. 2015;5:15173.
15. Chidembo A, Aboutalebi SH, Konstantinov K, Salari M, Winton B, Yamini SA, et al. Globular reduced graphene oxide-metal oxide structures for energy storage applications. Energy Environ Sci. 2012;5:5236–40.
16. Dideikin AT, Vul AY. Graphene oxide and derivatives: the place in graphene family. Front Phys. 2019;6:149.
17. Shareena TPD, McShan D, Dasmahapatra AK, Tchounwou PB. A review on graphene-based nanomaterials in biomedical applications and risks in environment and health. Nano-Micro Let. 2018;10:53.
18. Chung C, Kim Y-K, Shin D, Ryoo S-R, Hong BH, Min D-H. Biomedical applications of graphene and graphene oxide. Acc Chem Res. 2013;46:2211–24.
19. Peña-Bahamonde J, Nguyen HN, Fanourakis SK, Rodrigues DF. Recent advances in graphene-based biosensor technology with applications in life sciences. J Nanobiotechnol. 2018;16:75.
20. Lu Z, Chen X, Wang Y, Zheng X, Li CM. Aptamer based fluorescence recovery assay for aflatoxin B1 using a quencher system composed of quantum dots and graphene oxide. Microchim Acta. 2015;182:571–8.

21. Qu H, Csordas AT, Wang J, Oh SS, Eisenstein MS, Soh HT. Rapid and label-free strategy to isolate aptamers for metal ions. ACS Nano. 2016;10:7558–65.
22. Eissa S, Siddiqua A, Chinnappan R, Zourob MM. Electrochemical SELEX technique for the selection of DNA aptamers against the small molecule 11-deoxycortisol. ACS Appl Bio Mater. 2019.
23. Chinnappan R, Eissa S, Alotaibi A, Siddiqua A, Alsager OA, Zourob M. In vitro selection of DNA aptamers and their integration in a competitive voltammetric biosensor for azlocillin determination in waste water. Anal Chim Acta. 2020;1101:149–56.
24. Aljohani MM, Chinnappan R, Eissa S, Alsager OA, Weber K, Cialla-May D, et al. In vitro selection of specific DNA Aptamers against the anti-coagulant dabigatran etexilate. Sci Rep. 2018;8:13290.
25. Chinnappan R, Rahamn AA, AlZabn R, Kamath S, Lopata AL, Abu-Salah KM, et al. Aptameric biosensor for the sensitive detection of major shrimp allergen, tropomyosin. Food Chem. 2019;126133.
26. Chinnappan R, AlAmer S, Eissa S, Rahamn AA, Abu Salah KM, Zourob M. Fluorometric graphene oxide-based detection of Salmonella enteritis using a truncated DNA aptamer. Microchim Acta. 2017;185:61.
27. Tang Z, Parekh P, Turner P, Moyer RW, Tan W. Generating aptamers for recognition of virus-infected cells. Clin Chem. 2009;55:813–22.
28. Chinnappan R, AlZabn R, Abu-Salah KM, Zourob M. An aptamer based fluorometric microcystin-LR assay using DNA strand-based competitive displacement. Microchim Acta. 2019;186:435.
29. Chinnappan R, AlZabn R, Mir TA, Bader M, Zourob M. Fluorometric determination of okadaic acid using a truncated aptamer. Microchim Acta. 2019;186:406.
30. Alhadrami HA, Chinnappan R, Eissa S, Rahamn AA, Zourob M. High affinity truncated DNA aptamers for the development of fluorescence based progesterone biosensors. Anal Biochem. 2017;525:78–84.
31. Elshafey R, Siaj M, Zourob M. In vitro selection, characterization, and biosensing application of high-affinity cylindrospermopsin-targeting aptamers. Anal Chem. 2014;86:9196–203.
32. Vorobyeva MA, Davydova AS, Vorobjev PE, Pyshnyi DV, Venyaminova AG. Key aspects of nucleic acid library design for in vitro selection. Int J Mol Sci. 2018;19:470.
33. Komarova N, Kuznetsov A. Inside the black box: what makes SELEX better? Molecules. 2019;24:3598.
34. Ku T-H, Zhang T, Luo H, Yen TM, Chen P-W, Han Y, et al. Nucleic acid aptamers: an emerging tool for biotechnology and biomedical sensing. Sensors. 2015;15:16281–313.
35. Adachi T, Nakamura Y. Aptamers: a review of their chemical properties and modifications for therapeutic application. Molecules. 2019;24:4229.
36. Zhao Z, Chen H, Ma L, Liu D, Wang Z. A label-free electrochemical impedance aptasensor for cylindrospermopsin detection based on thionine-graphene nanocomposites. Analyst. 2015;140:5570–7.
37. Lei L, Peng L, Yang Y, Han B-p. Development of time-resolved fluoroimmunoassay for detection of cylindrospermopsin using its novel monoclonal antibodies. Toxins. 2018;10:255.
38. Díez-Quijada L, Guzmán-Guillén R, Prieto Ortega AI, Llana-Ruíz-Cabello M, Campos A, Vasconcelos V, et al. New method for simultaneous determination of microcystins and cylindrospermopsin in vegetable matrices by SPE-UPLC-MS/MS. Toxins. 2018;10:406.